A Relation between Fuel-optimal Low-thrust Trajectories and Two-body Orbits

IEPC-2015-95／ISTS-2015-b-95

Presented at Joint Conference of 30th International Symposium on Space Technology and Science 34th International Electric Propulsion Conference and 6th Nano-satellite Symposium, Hyogo-Kobe, Japan July 4 – 10, 2015

Shengxian Yu[1], Changyin Zhao, Rongyu Sun, Wei Zhang and Hongbo Wang

Purple Mountain Observatory, Chinese Academy of Sciences, Nanjing, 210000, China

Abstract: **Compared with other types of low-thrust trajectories, fuel-optimal low-thrust trajectories (bang-bang optimal control) problem is very difficult and complicated. Due to the existing thrusters are close to the ones with constant or given exhaust acceleration, this problem is worthy of studying and has important practical significances. In this paper, the relation between fuel-optimal low-thrust trajectory and two-body orbit is studied indirectly. The simplification into two-dimension case is made due to the complexity of the problem and the reason that most of the bodies in the solar system are close to the ecliptic plane. In order to obtain the relation, indirect method, homotopy method, shooting method and Pontryagin's minimum principle are employed to solve the fuel-optimal low-thrust problem jointly. Firstly, for any two transfer points in the space, the two-body orbit connects them can be obtained. Secondly, we give a change ($\Delta\vec{V}_0$) on the initial velocity, and test whether a probe with the new initial state can be transferred to the final state in the specified transfer time or not. It is surprising and inspiring that the feasible region of $\Delta\vec{V}_0$ is found to be regular. Finally, the parameters of the feasible region can be obtained by fitting numerically and the general expressions of the parameters which can be applied to any transfer orbits in the plane are presented.**

Nomenclature

a	=	semi-major axis
e	=	eccentricity
i	=	inclination
Ω	=	longitude of ascending node
ω	=	perigee longitude
M	=	mean anomaly
t_0, t	=	time
Δt	=	transfer time
$\vec{V}_0$	=	initial velocity of transfer orbit
$\Delta\vec{V}_0$	=	the variation of initial velocity
p	=	the major axis of an ellipse
q	=	the minor axis of an ellipse
φ	=	the phase angle of an ellipse

[1] Research assistant, Observational Center for Space Objects and Debris, yusx@pmo.ac.cn.

I. Introduction

THERE are some kinds of low-thrust trajectories, such as constant low-thrust trajectory, fuel-optimal low-thrust trajectory and energy-optimal low-thrust trajectory. The thrust of the third one is varying and continuous while the first two with constant or given exhaust thrust. As we all known, the existing thrusters are mostly the first two kinds of thrusts due to the reason that the third one is very hard to be implemented in the engineering. Therefore, it is meaningful to conduct a study on the first two kinds of low-thrust trajectories, especially the fuel-optimal low-thrust trajectory, which is more often used in the engineering. However, there is less research on the fuel-optimal low-thrust trajectory. People often use it as a tool to design deep space transfer trajectories instead. In this paper, the correlation between two-body orbit and fuel-optimal low-thrust trajectory is studied. It is helpful for us to understand the fuel-optimal low-thrust trajectory deeply and to design deep space trajectories purposefully.

Lee[4] obtained the Pareto front of the fuel and the flying time by coupling evolutionary algorithms and Lyapunov feedback control law (the Q-law), this updated numerical method is better than the normal Q-law in saving fuel and flying time. Fernandes[1] used Neighboring extremal algorithm to study the energy-optimal trajectory and the analytical expressions were deduced. Based on the linearization of the motion near reference orbits, Sukhanov[2] proposed a simple method for obtaining the transfer trajectories. Huang[3] used curve fitting in finding the correlation between the initial values of concomitant variables and the time escaped. Hence the approximate initial values of concomitant variables can be obtained by extrapolation to reduce the iterations.

In the paper, the problem about what kinds of orbits can be transferred to a specified state near a two-body orbit using low-thrust is studied by numerical method. Only the two-dimension case is considered due to the complexity and most of the bodies in the solar system are close to the ecliptic plane. Indirect method, homotopy method, shooting method and Pontryagin's minimum principle are employed to solve the fuel-optimal low-thrust problem jointly. Numerous numerical examples are made by varying the parameters using grid method, and then multiple least square methods are used to find the fitting result according to the model we establish.

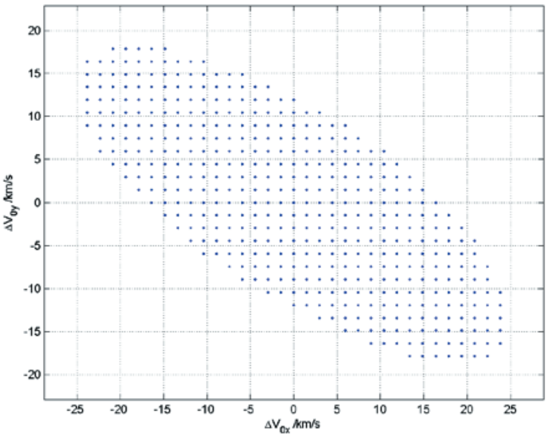

Figure 1. The feasible region of initial velocity.

II. The Feasible Region around the Initial State

A two-body orbit can be used as the nominal transfer orbit, such as the two-body Earth-to-Mars orbit whose initial orbital elements at time t_0 is as followed:

$$t_0: \quad a = 1.25\ AU, \quad e = 0.2, \quad i = 0^\circ, \qquad\qquad \Omega = 0^\circ, \quad \omega = 0^\circ, \quad M = 0^\circ. \tag{1}$$

The transfer time is specified to be Δt =255.231 d corresponding to a 180° transfer. The perturbation forces are ignored here. The position of the Earth is considered the same as Eq. (1) at time t_0. Therefore, the spacecraft departs from the Earth at time t_0 and then it will arrive at the Mars after a transfer time of Δt with no thrust.

The departure velocity is $\vec{V}_0$ which can be calculated from the orbital elements Eq. (1). In the paper, we keep the position $\vec{R}_0$ of the initial state unchanged, and alter the initial velocity to be $\vec{V}_0 + \Delta\vec{V}_0$. The magnitudes of $\Delta\vec{V}_0$ are given by grid method. For every magnitude of $\Delta\vec{V}_0$, the aim is to find out whether a spacecraft with the initial state $\left(\vec{R}_0, \vec{V}_0 + \Delta\vec{V}_0\right)$ can be transferred to the specified final state using fuel-optimal low-thrust.

For every magnitude of $\Delta\vec{V}_0$, we couple indirect method and homotopy method to verify whether the initial state $\left(\vec{R}_0, \vec{V}_0 + \Delta\vec{V}_0\right)$ and the final state can be connected by a fuel-optimal low-thrust trajectory. The magnitude of the low thrust used in this paper is specified as 0.12 N. A set of different $\Delta\vec{V}_0$ with a searching resolution of 1.489 km/s around the nominal initial state $\left(\vec{R}_0, \vec{V}_0\right)$ is tested and the feasible region of $\Delta\vec{V}_0$ is shown in Fig. 1. Each dot means an orbit in which a spacecraft can transfer from the initial state $\left(\vec{R}_0, \vec{V}_0+\Delta\vec{V}_0\right)$ to the final state using fuel-optimal low-thrust.

III. Curve Fitting of the Feasible Region

By changing the elements Ω, ω, M and transfer time Δt , the above process is repeated, it is obvious that the feasible region of initial velocity is independent of the elements Ω and ω . Hence, we only need to find out the correlation between the feasible region and the parameters e, M and Δt . As to its correlation with the semi-major axis a of the transfer orbit, it will be presented at last.

The outline of the feasible region shown in Fig. 1 is very close to an ellipse. Furthermore, all the other numerical results with different parameters e, M and Δt are also can be fitted by ellipse. Hence, we fit the result shown in Fig. 1 use the three parameters p, q and φ of an ellipse. They are the major axis, the minor axis and the phase angle of the ellipse respectively as shown in Fig. 2. The least square method is used to find the minimum ellipse that can include all the dots inside. The fitting result is as following:

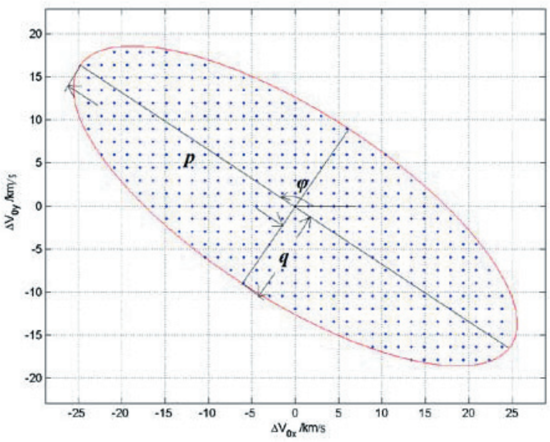

Figure 2. Ellipse fitting of the feasible region.

$$p = 29.69\ km/s,\ \ q{=}10.86\ km/s,\ \ \varphi = 2.5656\ rad \tag{2}$$

As stated above, the parameters p, q and φ are all correlated to e, M and Δt . Firstly, we vary the mean anomaly M from 0° to 360° with the step of 9° and keep the other two variables constants. The following correlations of p, q and $\varphi - M$ versus M are shown in Figs. 3-5.

These curves in Figs. 3-5 are very similar to sinusoid, so they can be fitted using the following functions:

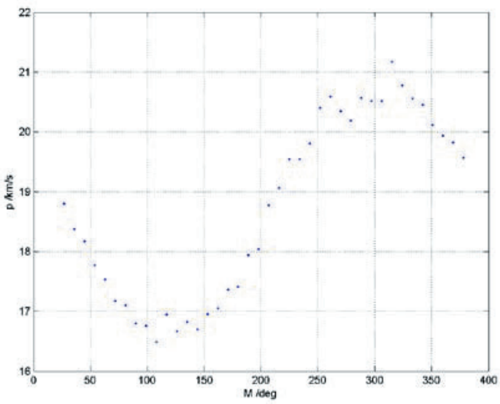

Figure 3. The parameter *p* versus *M*.

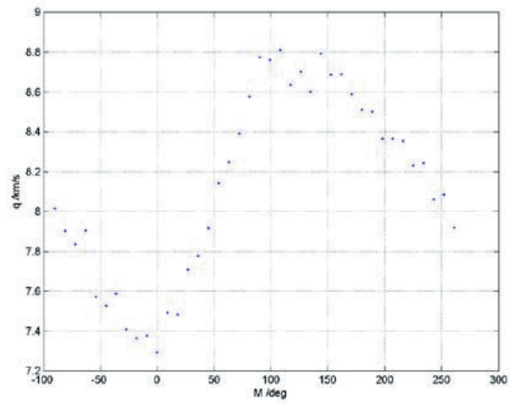

Figure 4. The parameter *q* versus *M*.

$$\begin{aligned} p &= p_0 + A_p \sin\left(M+\theta_p\right) \\ q &= q_0 + A_q \sin\left(M+\theta_q\right) \\ \varphi &= M + \varphi_0 + A_\varphi \sin\left(M+\theta_\varphi\right) \end{aligned} \tag{3}$$

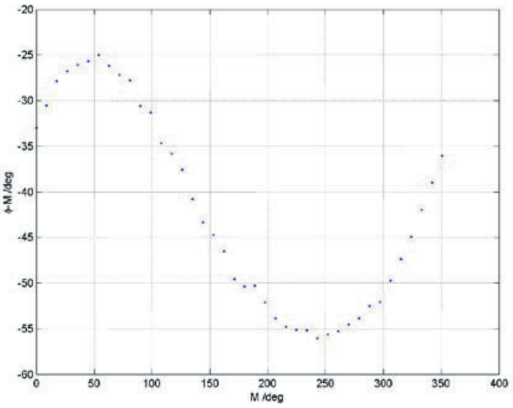

Figure 5. The parameter $\varphi - M$ versus *M*.

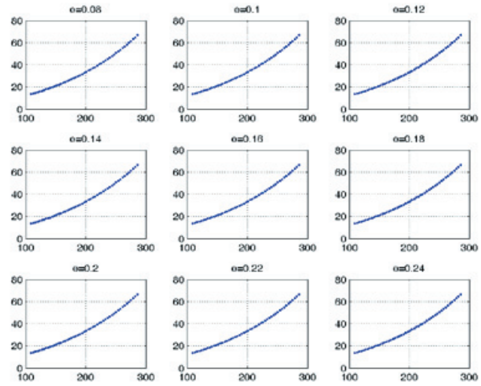

Figure 6. The variation of p_0 versus the transfer time Δt. The horizontal axis represents Δt (unit: deg), and the vertical axis represents p_0 (unit: km/s).

Secondly, the parameters (p_0, A_p, θ_p), (q_0, A_q, θ_q) and $(\varphi_0, A_\varphi, \theta_\varphi)$ in Eq. (3) are correlated to *e* and Δt. The magnitude of *e* is adopted from 0.08 to 0.24 with the step of 0.02, and Δt from 109.5 deg to 285.8 deg with the step of 3.526 deg. The results of (p_0, A_p, θ_p) versus *e* and Δt are displayed from Fig. 6 to Fig. 8.

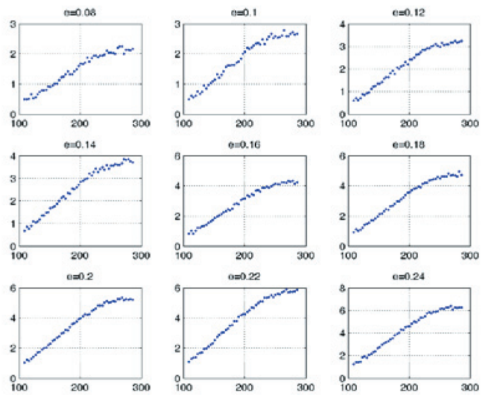

Figure 7. The variation of A_p versus the transfer time Δt. The horizontal axis represents Δt (unit: deg), and the vertical axis represents A_p (unit: km/s).

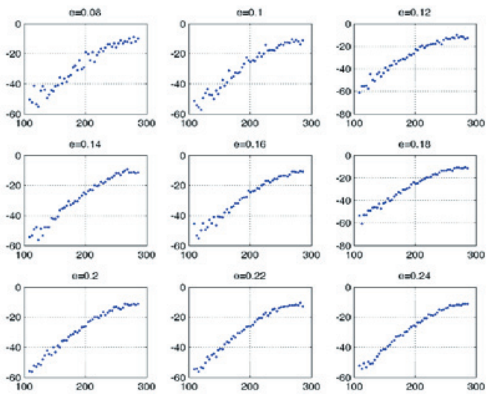

Figure 8. The variation of θ_p versus the transfer time Δt. The horizontal axis represents Δt (unit: deg), and the vertical axis represents θ_p (unit: deg).

As shown in Fig. 6 and Fig. 8, the parameters p_0 and θ_p are both independent of *e*, while A_p mainly shows a linear relation with *e*, so the following model is tried:

$$
\begin{aligned}
p_0 &= c_{10} + c_{11}\Delta t + c_{12}\Delta t^2 + c_{13}\Delta t^3 \\
A_p &= e\left(c_{20} + c_{21}\Delta t + c_{22}\Delta t^2 + c_{23}\Delta t^3\right) \\
\theta_p &= c_{30} + c_{31}\Delta t + c_{32}\Delta t^2 + c_{33}\Delta t^3
\end{aligned}
\tag{4}
$$

The other two sets of parameters (q_0, A_q, θ_q) and $(\varphi_0, A_\varphi, \theta_\varphi)$ show the same regularity with (p_0, A_p, θ_p), therefore Eq. (4) is also applicable to them.

The fitting results of these parameters are listed in table 1.

Table 1 The fitting results of c_{ij} (i=1~3, j=0~3).

c_{ij}	j=0	j=1	j=2	j=3
i=1 (km/s)	-0.729	7.013	-0.430	0.346
i=2 (km/s)	7.829	-13.297	7.976	-0.917
i=3 (rad)	1.963	-0.179	0.200	-0.025

The variables d_{ij} (i=1~3, j=0~3) and f_{ij} (i=1~3, j=0~3) are used to fit the other two sets of parameters, their results are listed in table 2 and table 3 respectively.

Table 2 The fitting results of d_{ij} (i=1~3, j=0~3).

d_{ij}	j=0	j=1	j=2	j=3
i=1 (km/s)	0.032	6.664	-1.426	0.166
i=2 (km/s)	-12.192	17.901	-6.041	0.666
i=3 (rad)	-3.156	2.167	-0.641	0.051

Table 3 The fitting results of f_{ij} (i=1~3, j=0~3).

f_{ij}	j=0	j=1	j=2	j=3
i=1 (km/s)	1.539	0.365	-0.030	0.001
i=2 (km/s)	2.728	-0.587	0.027	0.005
i=3 (rad)	-0.526	0.958	-0.253	0.019

If we take the results of the first curve fitting of p, q and φ (minimum ellipses include the feasible regions) as "observation data", the aim of the next two curve fittings using Eq. (3) and Eq. (4) is to approach the "observation data" p, q and φ using the parameters c_{ij}, d_{ij}, and f_{ij} (i=1~3, j=0~3). In order to assess the precision of the last two curve fittings, the RMS (root-mean-square) errors of the three parameters are given below:

$$RMS\left(p\right) = 0.35\ km/s,\ RMS\left(q\right) = 0.15\ km/s,\ RMS\left(\varphi\right) = 0.02\ rad \tag{5}$$

Compared with the searching resolution of 1.489 *km/s*, the RMS errors of the three parameters are much smaller and the fitting models are proved to be reasonable from this perspective.

As to how the results varied with the semi-major axis a of the transfer orbit, the following simple relationship is verified:

$$p(a) = (a/a_0)^{3/2}\,p(a_0),\quad q(a) = (a/a_0)^{3/2}\,q(a_0),\quad \varphi(a) = \varphi(a_0) \tag{6}$$

where a_0=1.25 AU, $p(a)$, $q(a)$ and $\varphi(a)$ mean the parameters corresponding to semi-major axis a. The parameter φ is independent of a.

IV. Verification of the Fitting Results

In this chapter, two numerical examples are presented. One is the example shown in Fig. 1 with the initial value of Eq. (1). It is used to verify the interpolation effect of our results obtained in the chapter 3. The other example adopts an initial state beyond the sample ranges. Its aim is to assess the applicability of the extrapolation of our results.

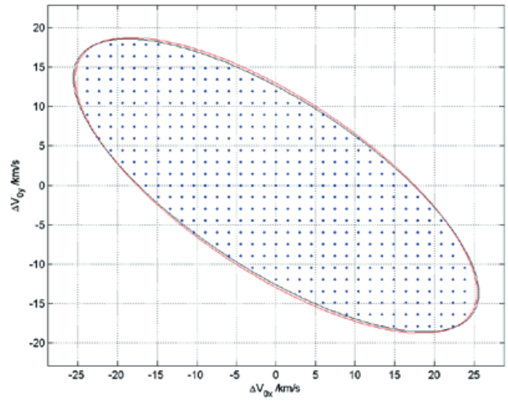

Figure 9. The fitting result of the feasible region.

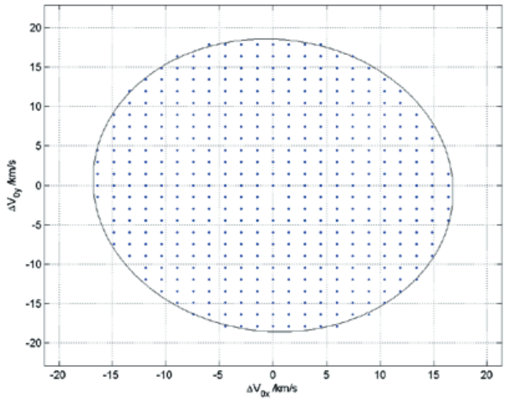

Figure 10. The fitting result of an extrapolated example.

The first example is presented in Fig. 9. The black solid line is the fitting results obtained from our model. It is obvious that the model seems to be reasonable and the fitting result is within an allowable error.

$$\begin{aligned} t_0: \quad & a = 2.0\ AU, \quad e = 0.3, \quad i = 0^\circ, \\ & \Omega = 0^\circ, \qquad \omega = 0^\circ, \quad M = 178.4772^\circ. \end{aligned} \tag{7}$$

the transfer time is $\Delta t = 85.4567 \deg$. The magnitudes of a, e and Δt are all beyond the sample ranges used in curve fitting before. The result obtained from our model is shown in Fig. 10. We can see that the feasible region is mainly inside the solid line and the error is smaller than the sample resolution. Therefore, it can be summarized that our model and method are both effective and the results are acceptable.

V. Conclusion

In the paper, indirect method, homotopy method, shooting method and Pontryagin's minimum principle are employed together to solve the fuel-optimal low-thrust trajectory jointly. A wealth of numerical examples are given to find the correlation between the feasible region which is the neighbourhood of the initial velocity and the parameters a, e, M and Δt. A model based on the numerical results is proposed, and multiple least square methods are made to obtain the parameters appear in the model. At last, two examples are performed to verify our model and method. The results show that the errors are within an acceptable magnitude. These prove that the model and method are reasonable and effective.

The results in this paper can be used in designing deep space trajectories. According to our results, whether a spacecraft with an initial state can be transfer to the specified final state can be judged quickly without numerical iteration.

References

Periodicals

[1]S. Da Silva Fernandes, W. A. Golfetto, "Numerical and Analytical Study of Optimal Low-Thrust Limited-Power Transfers between Close Circular Coplanar Orbits," *Mathematical Problems in Engineering*, Vol. 2007.

[2]A. A. Sukhanov, A. F. B. A. Prado, "Low-Thrust Orbital Transfers in the Two-Body Problem," *Mathematical Problems in Engineering*, Vol. 2012.

[3]Huang Hao, Han Chao, "Indirect Optimization of Low Thrust Escape Trajectories," *Chinese Space Science and Technology*, No.2, pp. 25-40, 2013.

Proceedings

[4]S. Lee, P. von Allmen, W. Fink, et. al., "Design and Optimization of Low-thrust Orbit Transfer," *Aerospace Conference*, 2005 IEEE, pp. 855-869.